Neuroradiology
https://doi.org/10.1007/s00234-018-2079-0

DIAGNOSTIC NEURORADIOLOGY

Combination of CT angiography and MRI in surgical planning of deep brain stimulation

Marie T. Krüger[1] · Volker A. Coenen[2] · Carolin Jenkner[3] · Horst Urbach[4] · Karl Egger[4] · Peter C. Reinacher[2]

Received: 23 December 2017 / Accepted: 13 August 2018

Abstract

Purpose For safe deep brain stimulation (DBS) planning, an accurate visualization and localization of vessels is mandatory. Contrast enhanced (ce) MRI depicts both arteries and veins. Computed tomography angiography (CTA) detects arteries with high geometric accuracy. We routinely combine both modalities for DBS planning.

Methods A total of 222 trajectories in a consecutive series of 113 patients who underwent DBS operations were included. In all trajectories, the number of veins and arteries in a 10-mm diameter around the planned trajectory were counted in a ceMRI and a CTA. If a vessel was visible in both modalities, the distance was measured.

Results A total of 370 vessels were counted. Two hundred forty vessels (65%) were visible in both modalities. With 134 of the vessels, we detected a difference of the vessel's location with an average distance of 1.24 mm (SD 0.58). Eighty vessels (22%) were visible only in the ceMRI, 50 vessels (13%) only in the CTA. We had four bleedings (1.8% per lead) of which one was symptomatic (0.45%).

Conclusion The majority of vessels were visible in both modalities; however, in more than half of these cases, the location was not identical. Here, the location in the CTA can be regarded as the ground truth. Moreover, both the CTA and the ceMRI depicted vessels not seen in the other imaging modality. We therefore assume that the combination of both imaging modalities for DBS planning increases the chance to detect vascular conflicts along the trajectory, thus reducing the risk of intracranial bleeding.

Keywords Deep brain stimulation · Computed tomography angiography · Contrast enhanced MRI · Intracranial bleeding

Introduction

Over the last 20 years, deep brain stimulation (DBS) has become a routinely performed neurosurgical procedure. The main DBS indications include Parkinson's disease, tremor, and dystonia, and a recent development has allowed the introduction of new indications such as psychiatric diseases [1, 2].

Intracranial bleeding caused by injuring intracranial vessels represents one of the major complications in DBS operations. This can lead to different kinds of hemorrhages ranging from intraparenchymal, intraventricular, epidural, and subarachnoid hemorrhage to venous infarction with secondary bleeding with an overall bleeding rate ranging from 1.4% to 3.4% for asymptomatic and 0.4% to 2.1% for symptomatic bleedings [3–12].

There are two fundamental requirements helping to minimize the risk for intracranial bleedings: (1) the accurate visualization of blood vessels (arteries and veins) and (2) their exact localization. A contrast enhanced MRI (ceMRI) can depict blood vessels, both arteries and veins, but the non-enhanced CT guarantees the high degree of accuracy.

The CTA combines both advantages by using the contrast medium to visualize the blood vessels (especially arteries) and the accuracy of a CT scan. For invasive EEG electrode placement, this method is already in use with good results [13, 14].

In our institution, we routinely perform a CTA instead of a non-enhanced CT scan on the day of surgery with the

✉ Peter C. Reinacher
peter.reinacher@uniklinik-freiburg.de

[1] Department of Neurosurgery, Medical Center - University of Freiburg, Faculty of Medicine, University of Freiburg, Freiburg, Germany

[2] Department of Stereotactic and Functional Neurosurgery, Medical Center - University of Freiburg, Faculty of Medicine, University of Freiburg, Freiburg, Germany

[3] Clinical Trials Unit, Medical Center - University of Freiburg, Faculty of Medicine, University of Freiburg, Freiburg, Germany

[4] Department of Neuroradiology, Medical Center - University of Freiburg, Faculty of Medicine, University of Freiburg, Freiburg, Germany

Published online: 22 August 2018

stereotactic frame attached. The scan is then fused with a ceMRI and T2 MRI on which target planning is performed. The aim of this study is to investigate if the combination of the ceMRI and the CTA in the planning of DBS operations can depict more blood vessels than one modality alone and if this reduces the bleeding rate when compared to the literature.

Patients and methods

Patients

A total of 129 consecutive patients, who underwent DBS operations from March 2014 to February 2017, were included in the study (Fig. 1). A ceMRI and a CTA were not performed in patients with poor thyroid or kidney function. They were also not performed on those who had allergies to the contrast enhancement medium, or for other reasons.

ceMRI

All patients received standard MRI 3D T2-weighted TSE (SPACE) and 3D T1-weighted fat saturated (fs) gradient echo (MP-RAGE) gadolinium enhanced sequences 1 or 2 days before surgery. Both sequences were acquired with a spatial resolution of 1 × 1 × 1 mm. The contrast agent, gadoteridol (ProHance©), at a dosage of 0.1 mmol (0.2 ml)/kg body weight, was used and administered intravenously with a flow of 1 ml/s.

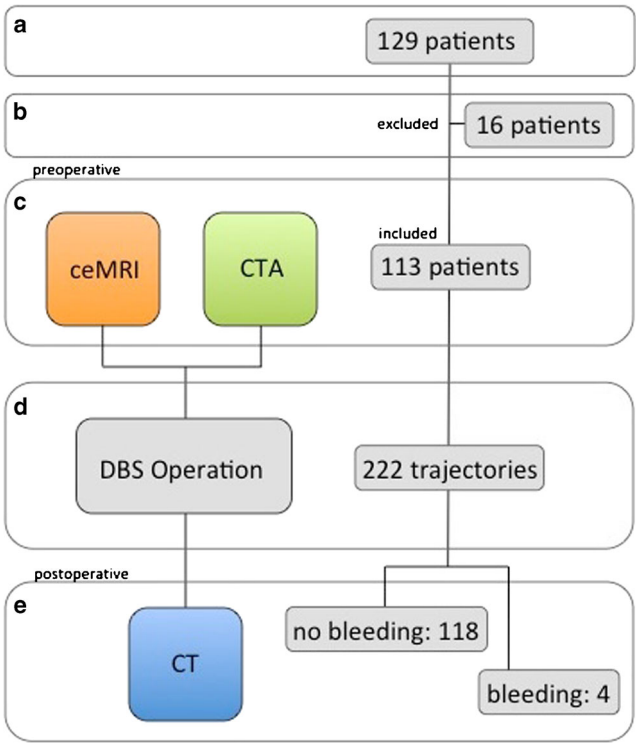

Fig. 1 Flow chart of the study. **a** One hundred twenty-nine consecutive patients were identified who had received the DBS operation. **b** Of these, 16 patients had to be excluded since no preoperative ceMRI or CTA was available. **c** One hundred thirteen patients with an available ceMRI and CTA were included. **d** In these patients, in a total of 22, 2 trajectories were performed in DBS operations. **e** Postoperative non-enhanced CT scans showed no bleeding in 118 trajectories and 4 bleedings in 4 trajectories

CTA

A CTA was performed on all patients on the day of surgery after placing a Leksell Frame G (Elekta, Stockholm, Sweden) under local anesthesia. In 58 patients, a CTA was performed using a 64-slice CT scanner (Siemens Definition AS, Erlangen, Germany), and in 55 patients, a CTA was conducted by using a 32-slice portable CT-scanner (BodyTom, Samsung/NeuroLogica, Danvers, USA). The contrast agent Iomeprol (Imeron©) 400 MCT was used in a dosage of 60 ml and was administered intravenously with a flow rate of 5 ml/s. Using the 64-slice scanner, the scan was started manually when the contrast media bolus was seen arriving in a premonitoring slice placed on the level of the circle of Willis. Using the BodyTom scanner, a CTA was performed with a fixed delay of 20-s post contrast media application start. No side effects were seen following the contrast media application.

CT

After surgery, in all patients, a non-enhanced control CT scan was performed on the 64-slice CT scanner to verify the final DBS electrode location and to rule out any postoperative intracranial hemorrhage.

Surgical procedure

Preplanning was performed on the day before surgery or on the day of surgery using Leksell SurgiPlan® (Elekta, Stockholm, Sweden) in 82 patients (163 trajectories) or FrameLink® (5.0, Medtronic SNT, Louisville, CO) in 31 patients (59 trajectories) planning systems.

The ceMRI and the CTA were matched, and the initially planned trajectory was adapted according to the new information from the CTA. The trajectory was always adjusted when, within the planned trajectory:

a) A vessel was depicted in the CTA that was not depicted in the ceMRI
b) A vessel was depicted in both modalities but with a deviation. In this case, the data from the CTA was taken into account due to its higher degree of accuracy. This principle was applied for either of the software systems.

Electrode placement was then carried out under local anesthesia while patients were awake in most cases (110 patients) or under general anesthesia (3 patients). In 43 patients, a

microelectrode recording (MER) was performed. An implantable pulse generator (IPG) was placed under general anesthesia either in the subclavicular or in the abdominal region during the same procedure.

All patients were operated on by two surgeons (V.C. or P.R.) in the same institution and with the same surgical methodology.

Evaluation

Data from the ceMRI and CTA were evaluated using either Leksell SurgiPlan® or FrameLink® planning systems. To compare the number of vessels depicted in the ceMRI and the CTA, a 10-mm-diameter circle was built around the trajectory (Figs. 2 and 3). The number of vessels found within this 10-mm-diameter circle was counted in both modalities. Four different variations were possible, and accordingly four different groups were built:

1) Group A: A vessel was found in the ceMRI but not in the CTA (Fig. 2).
2) Group B: A vessel was found in the CTA but not in the ceMRI (Figs. 2 and 3c, d).
3) Group C: A vessel was found in both modalities without deviation (Fig. 2; Fig. 3a, b)
4) Group D: A vessel found in both modalities with deviation (Fig. 2). In this case, the lateral distance in the plane perpendicular to the trajectory was measured. If a vessel was visible in more than one slice within the 10-mm-diameter circle, the slice with the lowest distance was analyzed. The step size during perpendicular trajectory inspection was 1.3 mm in Leksell SurgiPlan® and 1 mm in FrameLink®. For all vessels, their localization was documented to be in either of the four regions:

a) cortical in a sulcus
b) cortical but not in a sulcus
c) mesencephalic or
d) periventricular

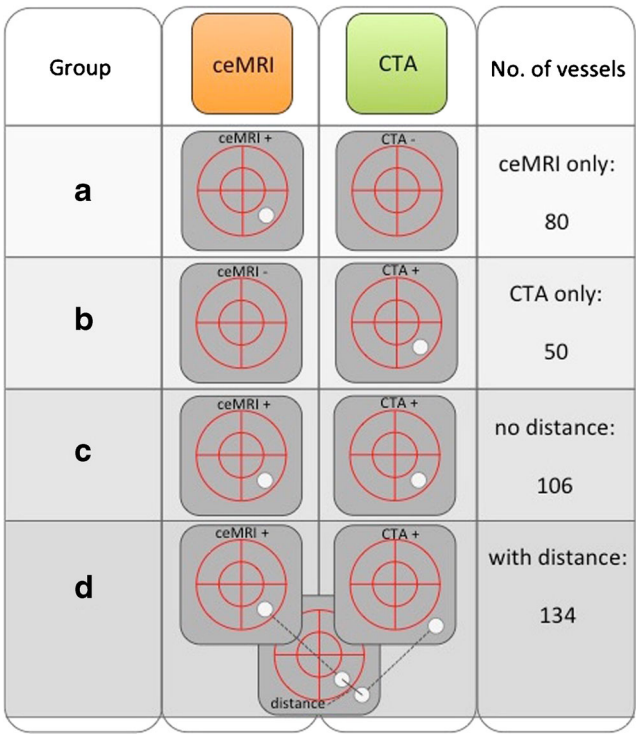

Fig. 2 Four different groups for vessel count in ceMRI and CTA. Group A: 80 vessels were detected in the ceMRI but not in the CTA; group B: 50 vessels were detected in the CTA but not in the ceMRI; group C: 106 vessels were detected in both modalities without deviation; group D: 134 vessels were detected in both modalities with deviation. The distance was then measured

Two observers performed the count. Bleedings were assessed volumetrically using Brainlab elements (Brainlab AG, Munich, Germany).

Statistical analysis

A descriptive analysis of the endpoints was performed as appropriate for the respective type of data (means, frequency tables). Two-sided 95% confidence intervals were calculated for several estimates.

Results

Patient data

In total, 16 of the 129 patients had to be excluded because they did not receive a preoperative CTA (10 patients) and/or ceMRI (6 patients) (Fig. 1).

Of the remaining 113 patients, 63 patients were male and 50 patients were female. Age ranged from 1 to 80 years (mean age = 55 years). The major target site was the nucleus subthalamicus (STN) in 54 cases (48%). In 43 (38%) of these cases, an intraoperative electrophysiology with microelectrode recording (MER) was performed. In the remaining 11 cases (10%), a posterior approach without MER was performed as previously described [15]. Other targets, all without MER, included the globus pallidus internus (GPi) in 31 cases (27%), the nucleus ventralis intermedius (Vim)/dentatorubrothalamic tract (DRT) in 21 cases (18%), the anterior thalamic nucleus (ATN) in 2 cases (2%), and the ventral posterior nucleus (VPN) of the thalamus in 3 cases (3%) as well as the superior lateral medial forebrain bundle (slMFB) in 2 cases (2%).

In 109 patients, 2 trajectories were planned, and in 4 patients, one trajectory was planned, resulting in a total number of 222 trajectories. In all these patients, a

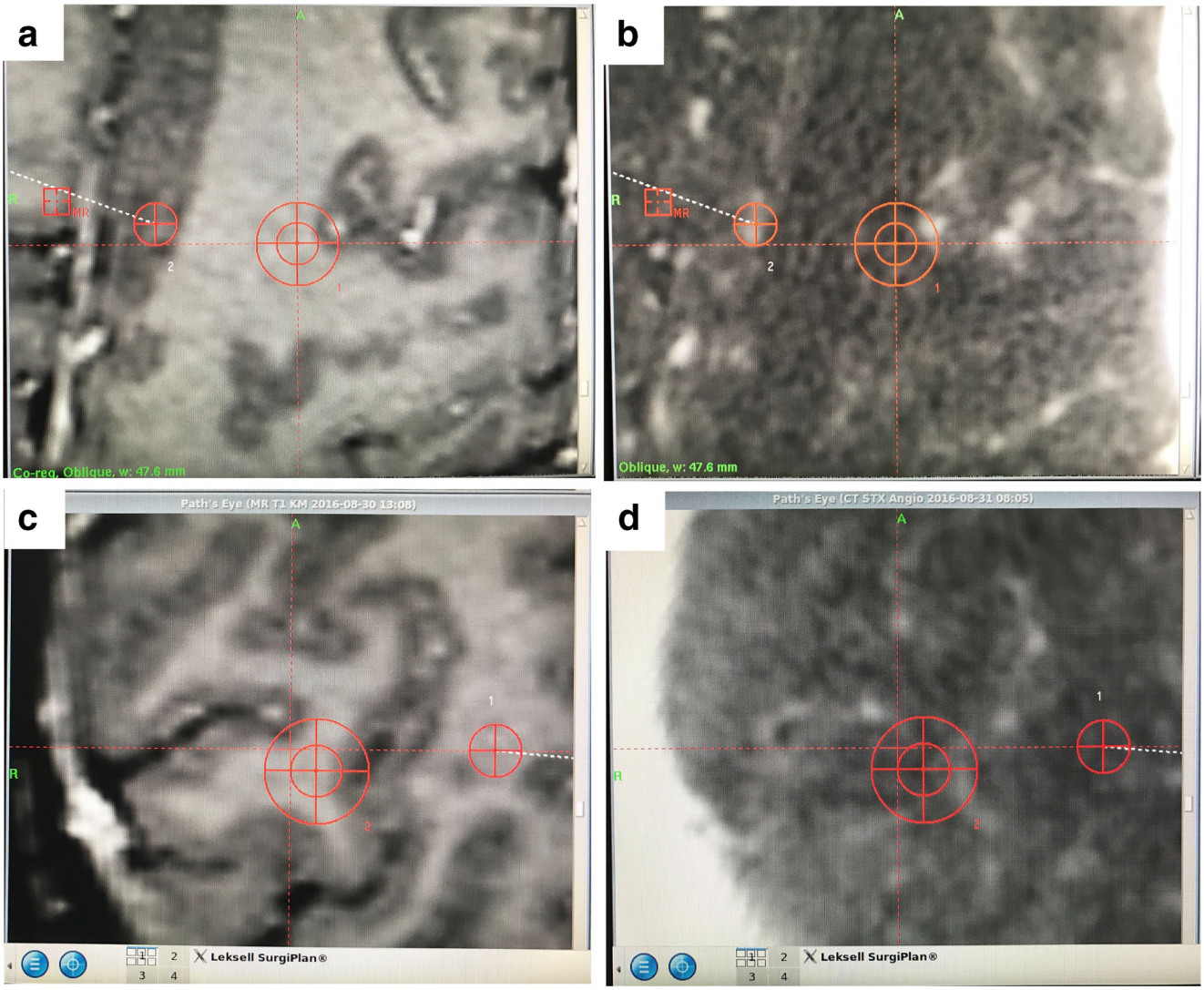

Fig. 3 Depiction of a vessel in the ceMRI and/or CTA. **a** The ceMRI shows a vessel within the 10-mm diameter. **b** The same vessel can be seen in the CTA. **c** The ceMRI shows no vessel within the 10-mm diameter. **d** In CTA, a vessel can be seen within the same 10-mm diameter

preoperative ceMRI, a CTA, and a postoperative non-enhanced CT scan were available.

Number of vessels in the ceMRI and the CTA within the 10-mm-diameter circle

A total of 370 vessels was counted in a total of 222 trajectories.

Of these 370 vessels, 80 vessels were visible in the ceMRI only (Fig. 2, group A; Table 1) and 50 vessels were visible in the CTA only (Fig. 2, group B; Table 1).

Two hundred forty vessels (65%) were visible in both modalities (Fig. 2, groups C and D; Table 1). Of these 240 vessels, 106 had no distance (group C) and 134 had a distance (group D).

When comparing both angiographic modalities (CTA and ceMRI) with only one angiographic method (ceMRI only or ceMRI and non-enhanced CT), at least one additional blood vessel was detected in 17.1% (CI [12.1; 22.1]) of the 222 trajectories (Table 2).

This means that an additional blood vessel can be detected in almost every sixth trajectory within a diameter of 10 mm of the planned target with the additional information given by the CTA.

Deviation of vessels in the ceMRI and the CTA

For the investigation of the distances of the blood vessels observed in the ceMRI and the CTA, only those blood vessels found in both modalities were considered (groups C and D). One hundred thirty-four of a total of 240 blood vessels found in both modalities had a distance greater 0 (group D). The mean distance for those blood vessels was 1.24 mm (CI [1.14, 1.34], $n = 134$). The mean distance for all 240 blood

Table 1 A total of 320 blood vessels were visible in the ceMRI and the CTA whereas only 80 were visible in the ceMRI and only 50 were visible in the CTA

No. of vessels in ceMRI	No. of vessels in CTA	No. of vessels in both ceMRI and CTA
Total: 320	290	240
ceMRI only: 80 (group A)	CTA only: 50 (group B)	No distance: 106 (group C)
		With distance: 134 (group D)

vessels including those with distance 0 was 0.69 mm (CI [0.59, 0.79], $n = 240$).

Localization of vessels in the ceMRI and CTA

The majority of all vessels counted within a 10-mm diameter around the planned trajectory was found periventricular (43%), followed by the cortical region in a sulcus (24%), mesencephalic (17%), and cortical outside a sulcus (16%) (Table 3). Most vessels found in both modalities showed a deviation in the periventricular and mesencephalic region (85% vs. 15%), whereas no distance was found mostly in the cortical region (72% vs. 28%) (Table 3). When looking at those vessels found only in the ceMRI or only in the CTA, the most deviations were seen in the periventricular and cortical sulcus region. The ceMRI depicted most vessels periventricularly (55%), whereas the CTA depicted most vessels in the cortex region close to a sulcus (38%).

Intracranial bleedings

The postoperative CT scans showed bleedings in three patients (Fig. 4). In two patients, the bleeding was unilateral, and in one patient the bleeding was bilateral (1.8% per lead).

One of the unilateral bleedings was a minimal ventricular bleeding in a 61-year-old male patient. He underwent DBS for Parkinson's disease, and the STN was targeted via a posterior approach without performing an MER (Fig. 4a). The patient did not develop any neurological deficits.

Table 2 In 184 of 222 trajectories, no additional blood vessel was detected in the additional CTA. In 29 trajectories (13.1%), one additional vessel was seen; in six trajectories (2.7%), two additional vessels and in three trajectories (1.3%) three additional vessels were found. Thus, in 17.1% of all trajectories, at least one additional vessel was detected in the additional CTA as compared to ceMRI only

Additional detected blood vessels in ceMRI + CTA compared to ceMRI only	Trajectories	%	%
0	184	82.9	82.9
1	29	13.1	17.1
2	6	2.7	
3	3	1.3	
Total	222	100	100

The second unilateral bleeding occurred in a 62-year-old male with Parkinson's disease. The STN was targeted, and an MER was performed. The bleeding was localized in the right thalamus close to the lead with a volume of 1.36 cm^3 (Fig. 4c). The patient presented with confusion and disorientation immediately after surgery. However, the symptoms improved over the course of the next few days and he was discharged after 14 days with only mild symptoms. During his out-patient visit 3 months later, he had fully recovered from symptoms and the hematoma was no longer visible on the CT scan.

The third intracranial hemorrhage occurred in a 60-year-old male patient with Parkinson's disease and STN as a target, where an MER was performed. The CT scans showed small bilateral bleedings with volumes of 1.81 cm^3 and 0.35 cm^3 (Fig. 4, B). This patient did not develop any neurological deficits.

Retrospectively we did not find any vessels in the ceMRI or the CTA that could explain any of the bleedings.

Discussion

DBS is a highly elective surgical procedure, and therefore, the prevention of complications should be of paramount importance. The visualization and exact localization of blood vessels, both arteries and veins, plays a fundamental role in minimizing the risk of intracranial bleedings.

The ceMRI offers the advantage of high anatomic resolution and depicts both arteries and veins, but is inherent to image distortion. However, with this method numerous vessels are still not depicted [14, 16]. For the planning of stereo-electroencephalography (sEEG) operations, an additional angiography is therefore often performed [17, 18]. However, this method itself is invasive, holding many risks by the procedure itself [19, 20].

An MRI scan improves trajectory planning due to its high anatomical resolution. In many centers, the complete planning is performed with an MRI [7, 21–23] only, which is conducted with the frame attached to the patient's head. In this case, the only visualization and information on the localization of blood vessels is given by the ceMRI sequences.

Alternatively many centers perform the trajectory planning on an MRI scan including a ceMRI to depict blood vessels and match it with a non-enhanced CT scan, performed with the frame attached [3, 7, 25–28]. In stereotactic procedures, a CT

Table 3 Distribution of the counted vessels within a 10-mm diameter of the planned trajectory, in the cortical region within and away from a sinus, mesencephalic and periventricular. This distribution is provided for vessels found in ceMRI and CTA only as well as in both modalities with and without a distance

Group	Total	Cortical sulcus total	Cortical no sulcus total	Mesencephalic total	Periventricular total
A (ceMRI only)	80	13	12	11	44
B (CTA only)	50	19	11	10	10
C (no distance)	106	45	31	16	14
D (with distance)	134	13	7	27	87
All groups	370	90	61	64	155

scan is commonly considered ground truth for accuracy [24, 25]; however, the two modalities (ceMRI an CT) then need to be fused. This image fusion is a source of inaccuracy. Still, the visualization and information on the localization of blood vessels is only given by the ceMRI sequences.

A CTA combines the advantages of the depiction of blood vessels and the accuracy of a CT scan. In the field of sEEG surgery, a CTA is therefore often performed. This method has been described to depict significantly more vessels than a ceMRI, yet without the invasive character of a DSA [14].

In this study, we combined both modalities (ceMRI and CTA) during the planning of DBS trajectories. We were able to show that with the additional information given by the CTA, at least one additional blood vessel could be detected in 17.1% of the 222 trajectories. This means that in every sixth trajectory, an additional vessel could be detected and included into the trajectory planning.

Furthermore, we found that in more than half of the cases where a blood vessel was visible in both modalities (groups C and D), the mean distance between them was 1.24 mm. This error could be caused by a geometrical inaccuracy of the MRI image and the fusion step. Since the CT scan is considered the ground truth for accuracy, one should regard the vessels depicted in the CTA as the "true" localization and consider changing the preplanned trajectory according to the new information given by the CTA. This inaccuracy was most often observed for vessels depicted in the mesencephalic and periventricular region, making the additional CTA specifically relevant for this critically deep region. Furthermore, when looking at the distribution of vessels found in each modality, the ceMRI depicts more vessels in the periventricular region, whereas the CTA shows more vessels in the cortical region, indicating once more, that both methods complement one another.

The aim of the described efforts to visualize blood vessels in the surgical planning system is to reduce the rate of intracranial bleedings. In comparable studies (more than 100 patients, postoperative CT or MRI scans, no exclusion concerning size or type of bleeding), the bleeding rates ranged from 1.4% to 3.3% per lead (mean 2.8%) for symptomatic and asymptomatic bleedings [3–6, 9, 11]. Thus, the hemorrhage rate of 1.8% reported in this study is among the lowest. In the symptomatic bleedings, rates ranged from 0.6% to 2.1% per lead (mean 1.5%) [3–6, 8–11]; again, our rate of 0.45% is

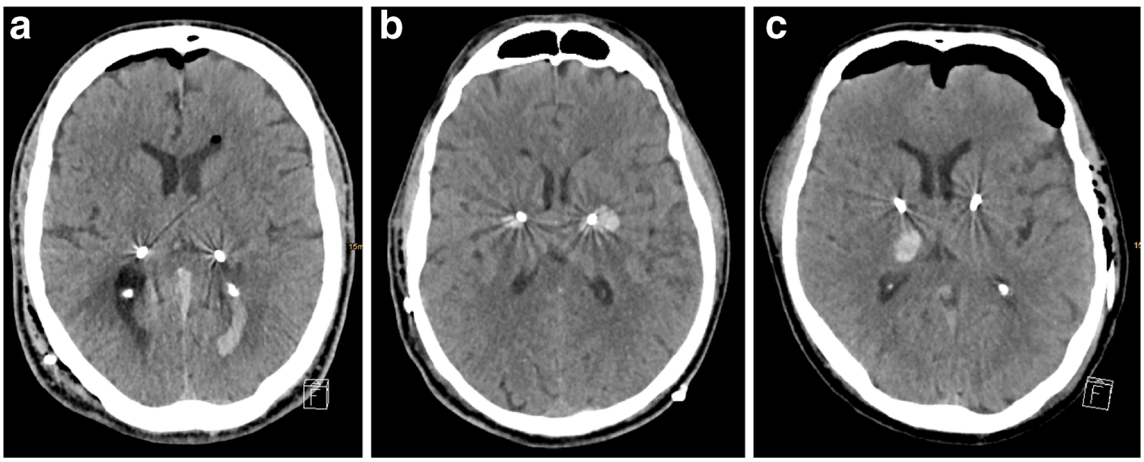

Fig. 4 Bleedings after implantation of leads. **a** Ventricular bleeding in a patient with STN target via a posterior approach. **b** Bilateral bleeding and **c** unilateral bleeding in patients with STN target

among the lowest compared to the literature. Moreover, we did not find any complications caused by the additional contrast medium applied to our patients.

The most important limitation of this study lies in its retrospective design, including an analysis of only one cohort of patients studied with a CTA. Since we did not compare our results with any other technique such as non-enhanced CT scans or MR angiography, there is no direct control group. The comparison of our results with data from the literature, therefore, only allows us to state our conclusion of a reduced bleeding risk with the combination of both modalities as an assumption rather than a clear correlation. Furthermore, retrospectively, we were not able to state the exact number of trajectories that was changed due to the additional information received by the CTA in total or in either of the two software planning systems used.

The results in this study show that ceMRI and CTA are complementary techniques. Their combination can increase the detection rate of blood vessels and can improve their localizations, thus contributing to a reduction of the risk for intracranial bleeding in deep brain stimulation operations. The advantages of both modalities can therefore also be used during other stereotactic surgeries such as biopsies and sEEG-implantations.

Acknowledgments We thank Olivia Chorny for reviewing the manuscript and providing language support.

Compliance with ethical standards

Conflict of interest The authors declare that they have no conflict of interest.

Ethical approval All procedures performed in studies involving human participants were in accordance with the ethical standards of the institutional research committee and with the 1964 Helsinki declaration and its later amendments or comparable ethical standards. For this type of study formal consent is not required.

Informed consent For this type of retrospective study formal consent is not required.

References

1. Schuepbach WMM, Rau J, Knudsen K, Volkmann J, Krack P, Timmermann L, Hälbig TD, Hesekamp H, Navarro SM, Meier N, Falk D, Mehdorn M, Paschen S, Maarouf M, Barbe MT, Fink GR, Kupsch A, Gruber D, Schneider GH, Seigneuret E, Kistner A, Chaynes P, Ory-Magne F, Brefel Courbon C, Vesper J, Schnitzler A, Wojtecki L, Houeto JL, Bataille B, Maltête D, Damier P, Raoul S, Sixel-Doering F, Hellwig D, Gharabaghi A, Krüger R, Pinsker MO, Amtage F, Régis JM, Witjas T, Thobois S, Mertens P, Kloss M, Hartmann A, Oertel WH, Post B, Speelman H, Agid Y, Schade-Brittinger C, Deuschl G, EARLYSTIM Study Group (2013) Neurostimulation for Parkinson's disease with early motor complications. N Engl J Med 368:610–622. https://doi.org/10.1056/NEJMoa1205158
2. Schlaepfer TE, Bewernick BH, Kayser S, Hurlemann R, Coenen VA (2014) Deep brain stimulation of the human reward system for major depression—rationale, outcomes and outlook. Neuropsychopharmacology 39:1303–1314. https://doi.org/10.1038/npp.2014.28
3. Ben-Haim S, Asaad WF, Gale JT, Eskandar EN (2009) Risk factors for hemorrhage during microelectrode-guided deep brain stimulation and the introduction of an improved microelectrode design. Neurosurgery 64:754–763. https://doi.org/10.1227/01.NEU.0000339173.77240.34
4. Binder DK, Rau G, Starr PA (2004) Hemorrhagic complications of microelectrode-guided deep brain stimulation. Stereotact Funct Neurosurg 80:28–31. https://doi.org/10.1159/000075156
5. Binder DK, Rau GM, Starr PA (2005) Risk factors for hemorrhage during microelectrode-guided deep brain stimulator implantation for movement disorders. Neurosurgery 56:722–732 discussion 722–732
6. Seijo FJ, Alvarez-Vega MA, Gutierrez JC, Fdez-Glez F, Lozano B (2007) Complications in subthalamic nucleus stimulation surgery for treatment of Parkinson's disease. Review of 272 procedures. Acta Neurochir 149:867–876. https://doi.org/10.1007/s00701-007-1267-1
7. Terao T, Takahashi H, Yokochi F, Taniguchi M, Okiyama R, Hamada I (2003) Hemorrhagic complication of stereotactic surgery in patients with movement disorders. J Neurosurg 98:1241–1246. https://doi.org/10.3171/jns.2003.98.6.1241
8. Voges J, Hilker R, Bötzel K, Kiening KL, Kloss M, Kupsch A, Schnitzler A, Schneider GH, Steude U, Deuschl G, Pinsker MO (2007) Thirty days complication rate following surgery performed for deep-brain-stimulation. Mov Disord 22:1486–1489. https://doi.org/10.1002/mds.21481
9. Patel DM, Walker HC, Brooks R, Omar N, Ditty B, Guthrie BL (2015) Adverse events associated with deep brain stimulation for movement disorders analysis of 510 consecutive cases. Oper Neurosurg 11:190–199. https://doi.org/10.1227/NEU.0000000000000659
10. Sansur CA, Frysinger RC, Pouratian N, Fu KM, Bittl M, Oskouian RJ, Laws ER, Elias WJ (2007) Incidence of symptomatic hemorrhage after stereotactic electrode placement. J Neurosurg 107:998–1003. https://doi.org/10.3171/JNS-07/11/0998
11. Chen T, Mirzadeh Z, Chapple K, Lambert M, Ponce FA (2016) Complication rates, lengths of stay, and readmission rates in "awake" and "asleep" deep brain simulation. J Neurosurg 127:1–10. https://doi.org/10.3171/2016.6.JNS152946
12. Wang X, Wang J, Zhao H, Li N, Ge S, Chen L, Li J, Jing J, Su M, Zheng Z, Zhang J, Gao G, Wang X (2016) Clinical analysis and treatment of symptomatic intracranial hemorrhage after deep brain stimulation surgery. Br J Neurosurg 0:1–6. doi: https://doi.org/10.1080/02688697.2016.1244252, 31
13. Nowell M, Rodionov R, Diehl B, Wehner T, Zombori G, Kinghorn J, Ourselin S, Duncan J, Miserocchi A, McEvoy A (2014) A novel method for implementation of frameless StereoEEG in epilepsy surgery. Neurosurgery 10:525–534. https://doi.org/10.1227/NEU.0000000000000544
14. Gilard V, Proust F, Gerardin E, Lebas A, Chastan N, Fréger P, Parain D, Derrey S (2016) Usefulness of multidetector-row computerized tomographic angiography for the surgical planning in stereoelectroencephalography. Diagn Interv Imaging 97:333–337. https://doi.org/10.1016/j.diii.2015.10.001
15. Coenen VA, Rijntjes M, Prokop T, Piroth T, Amtage F, Urbach H, Reinacher PC (2016) One-pass deep brain stimulation of dentato-rubro-thalamic tract and subthalamic nucleus for tremor-dominant or equivalent type Parkinson's disease. Acta Neurochir 158:773–781. https://doi.org/10.1007/s00701-016-2725-4

16. Gonzalez-Martinez J, Mullin J, Vadera S, Bulacio J, Hughes G, Jones S, Enatsu R, Najm I (2014) Stereotactic placement of depth electrodes in medically intractable epilepsy. J Neurosurg 120:639–644. https://doi.org/10.3171/2013.11.JNS13635
17. Blatt DR, Roper SN, Friedman WA (1997) Invasive monitoring of limbic epilepsy using stereotactic depth and subdural strip electrodes: surgical technique. Surg Neurol 48:74–79. https://doi.org/10.1016/S0090-3019(96)00277-7
18. Burneo JG, Steven DA, McLachlan RS, Parrent AG (2006) Morbidity associated with the use of intracranial electrodes for epilepsy surgery. Can J Neurol Sci J Can Sci Neurol 33:223–227
19. Guenot M, Isnard J, Ryvlin P, Fischer C, Ostrowsky K, Mauguiere F, Sindou M (2001) Neurophysiological monitoring for epilepsy surgery: the Talairach SEEG method. Stereotact Funct Neurosurg 77:29–32. https://doi.org/10.1159/000064595
20. Behrens E, Schramm J, Zentner J, König R (1997) Surgical and neurological complications in a series of 708 epilepsy surgery procedures. Neurosurgery 41:1–9 discussion 9–10
21. Østergaard K, Sunde N, Dupont E (2002) Effects of bilateral stimulation of the subthalamic nucleus in patients with severe Parkinson's disease and motor fluctuations. Mov Disord 17:693–700. https://doi.org/10.1002/mds.10188
22. Starr PA, Christine CW, Theodosopoulos PV, Lindsey N, Byrd D, Mosley A, Marks WJ Jr (2002) Implantation of deep brain stimulators into subthalmic nucleus: technical approach and magnetic imaging—verified electrode locations. J Neurosurg 97:370–387. https://doi.org/10.3171/jns.2002.97.2.0370
23. Sterio D, Zonenshayn M, Mogilner AY et al (2002) Neurophysiological refinement of subthalamic nucleus targeting. Neurosurgery 50:58–67 discussion 67–69
24. Voges J, Volkmann J, Allert N, Lehrke R, Koulousakis A, Freund HJ, Sturm V (2002) Bilateral high-frequency stimulation in the subthalamic nucleus for the treatment of Parkinson disease: correlation of therapeutic effect with anatomical electrode position. J Neurosurg 96:269–279. https://doi.org/10.3171/jns.2002.96.2.0269
25. Rezai AR, Machado AG, Deogaonkar M, Azmi H, Kubu C, Boulis NM (2008) Surgery for movement disorders. Neurosurgery 62:SHC809–SHC839. https://doi.org/10.1227/01.neu.0000316285.52865.53